A LETTERS JOURNAL EXPLORING
THE FRONTIERS OF PHYSICS

OFFPRINT

Dynamics of a linear magnetic “microswimmer molecule”

S. BABEL, H. LÖWEN and A. M. MENZEL

EPL, **113** (2016) 58003

Please visit the website
`www.epljournal.org`

Note that the author(s) has the following rights:
– immediately after publication, to use all or part of the article without revision or modification, **including the EPLA-formatted version**, for personal compilations and use only;
– no sooner than 12 months from the date of first publication, to include the accepted manuscript (all or part), **but not the EPLA-formatted version**, on institute repositories or third-party websites provided a link to the online EPL abstract or EPL homepage is included.
For complete copyright details see: `https://authors.epletters.net/documents/copyright.pdf`.

epl

A LETTERS JOURNAL EXPLORING
THE FRONTIERS OF PHYSICS

AN INVITATION TO SUBMIT YOUR WORK

www.epljournal.org

The Editorial Board invites you to submit your letters to EPL

EPL is a leading international journal publishing original, innovative Letters in all areas of physics, ranging from condensed matter topics and interdisciplinary research to astrophysics, geophysics, plasma and fusion sciences, including those with application potential.

The high profile of the journal combined with the excellent scientific quality of the articles ensures that EPL is an essential resource for its worldwide audience. EPL offers authors global visibility and a great opportunity to share their work with others across the whole of the physics community.

Run by active scientists, for scientists

EPL is reviewed by scientists for scientists, to serve and support the international scientific community. The Editorial Board is a team of active research scientists with an expert understanding of the needs of both authors and researchers.

www.epljournal.org
epl
ISSN 0295-5075
A Letters Journal Exploring
the Frontiers of Physics
Volume 105 Number 1
January 2014

www.epljournal.org
epl
ISSN 0295-5075
A Letters Journal Exploring
the Frontiers of Physics
Volume 104 Number 1
October 2013

www.epljournal.org
epl
ISSN 0295-5075
A Letters Journal Exploring
the Frontiers of Physics
Volume 103 Number 1
July 2013

www.epljournal.org

epl A Letters Journal Exploring the Frontiers of Physics

www.epljournal.org

OVER
560,000
full text downloads in 2013

24 DAYS
average accept to online publication in 2013

10,755
citations in 2013

"We greatly appreciate the efficient, professional and rapid processing of our paper by your team."

Cong Lin
Shanghai University

Six good reasons to publish with EPL

We want to work with you to gain recognition for your research through worldwide visibility and high citations. As an EPL author, you will benefit from:

1. **Quality** – The 50+ Co-editors, who are experts in their field, oversee the entire peer-review process, from selection of the referees to making all final acceptance decisions.
2. **Convenience** – Easy to access compilations of recent articles in specific narrow fields available on the website.
3. **Speed of processing** – We aim to provide you with a quick and efficient service; the median time from submission to online publication is under 100 days.
4. **High visibility** – Strong promotion and visibility through material available at over 300 events annually, distributed via e-mail, and targeted mailshot newsletters.
5. **International reach** – Over 2600 institutions have access to EPL, enabling your work to be read by your peers in 90 countries.
6. **Open access** – Articles are offered open access for a one-off author payment; green open access on all others with a 12-month embargo.

Details on preparing, submitting and tracking the progress of your manuscript from submission to acceptance are available on the EPL submission website **www.epletters.net**.

If you would like further information about our author service or EPL in general, please visit **www.epljournal.org** or e-mail us at **info@epljournal.org**.

EPL is published in partnership with:

EPS
European Physical Society

Società Italiana di Fisica
Società Italiana di Fisica

edp sciences
EDP Sciences

IOP Publishing
IOP Publishing

www.epljournal.org

A Letters Journal Exploring
the Frontiers of Physics

March 2016

EPL, **113** (2016) 58003
doi: 10.1209/0295-5075/113/58003

www.epljournal.org

Dynamics of a linear magnetic “microswimmer molecule”

S. Babel, H. Löwen and A. M. Menzel

Institut für Theoretische Physik II: Weiche Materie, Heinrich-Heine-Universität Düsseldorf - Universitätsstraße 1, D-40225 Düsseldorf, Germany

received 12 November 2015; accepted in final form 18 March 2016
published online 31 March 2016

PACS 82.70.Dd – Colloids
PACS 47.63.Gd – Swimming microorganisms
PACS 47.20.Ky – Nonlinearity, bifurcation, and symmetry breaking

Abstract – In analogy to nanoscopic molecules that are composed of individual atoms, we consider an active “microswimmer molecule”. It is made of three individual magnetic colloidal microswimmers that are connected by harmonic springs and interact hydrodynamically. In the ground state, they form a linear straight molecule. We analyze the relaxation dynamics for perturbations of this straight configuration. As a central result, with increasing self-propulsion, we observe an oscillatory instability in accord with a subcritical Hopf bifurcation scenario. It is accompanied by a corkscrew-like swimming trajectory of increasing radius. Our results can be tested experimentally, using, for instance, magnetic self-propelled Janus particles, supposably linked by DNA molecules.

Copyright © EPLA, 2016

Introduction. – Often, self-propelled objects are realized on the colloidal level in the form of active microswimmers [1,2]. Examples are Janus particles selectively heated [3,4] or catalyzing chemical reactions [5,6] on one of their hemispheres, or representatives of nature in the form of swimming microorganisms [7]. As witnessed by several reviews [1,2,8,9], the migration behavior of individual self-propelled particles has been studied intensely. If not guided from outside, the long-term translation dynamics of individual self-propelled particles appears diffusive due to fluctuations [5]. In contrast to that, interactions between many self-propelled objects can induce directed collective motion [10–12]. Steric [13,14] or elastic [15–18] interactions are sufficient for this purpose.

It is now time to extend the hitherto conception, where individual microswimmers serve as the immediate building blocks of active matter, to a more hierarchical approach. In passive equilibrium, just as atoms form nanoscopic molecules, individual colloidal particles were combined to “colloidal molecules” [19–21]. Here, we address active systems. We introduce the effect of *permanent elastic bonds* between individual microswimmers, such that they form a self-propelled colloidal “*microswimmer molecule*”. This is different from phoretically stabilized aggregates of catalytically active, not necessarily self-propelled colloidal particles [22–24] or clusters of active dipolar particles [25].

At present, we investigate the stability of the directed motion of one colloidal microswimmer molecule. Three individual microswimmers, active spherical particles in our case, are linearly connected by harmonic springs, see fig. 1. We stress that each individual sphere represents a microswimmer by itself, *e.g.* an active Janus particle [3–6], and already propels by itself. For previously studied three-bead swimmers [26–28], net motion results from imposed relative velocities between the individual beads, possibly induced by active deformations of the links. Our springs are passive. Since in our case each individual sphere represents a torque-free straight-moving microswimmer, only their overall (possibly static) orientational ordering determines the overall motion of the molecule, in contrast to previously discussed synchronization problems [29–31]. To stabilize a linear straight alignment of the molecule, we assign a dipolar magnetic moment to each sphere, inspired by active magnetic Janus particles [32]. Differently from magnetically activated microswimmers [33–35], our magnetic interactions only have a (static) stabilizing effect. The coupling to magnetic effects and the possibility of a truly three-dimensional destabilization further distinguishes our approach from the models in refs. [26–28].

Each of our spherical swimmers acts on the surrounding fluid in the form of a force dipole [36]. That is, two little-distanced force centers apply antiparallel forces of equal magnitude onto the fluid, setting it into motion. If the sphere is asymmetrically located with respect to its self-induced fluid flow, it experiences a net drag and is driven forward [37,38]. Through the self-induced fluid flows, our three linked spherical swimmers hydrodynamically interact. As a central result, we find that

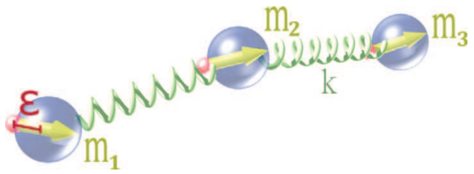

Fig. 1: (Color online) Simplified magnetic colloidal microswimmer molecule, here slightly perturbed out of the aligned straight ground state. Three active spherical swimmers are linked by harmonic springs of spring constant k. On each swimmer, an active force dipole acts on the surrounding fluid, shifted out of the center by a distance ε along the magnetic moment $\boldsymbol{m}_i$ ($i = 1, 2, 3$). In the depicted case of $\varepsilon < 0$ we set $\sigma_0 > 0$ for the strength of the active drive (pusher); for $\varepsilon > 0$ the active centers are shifted towards the heads of the vectors $\boldsymbol{m}_i$ and we set $\sigma_0 < 0$ (puller).

straight configurations of the overall molecule and straight trajectories become unstable above a certain strength of self-propulsion. Above this threshold, an oscillatory (Hopf-like) instability resulting in corkscrew-like motion arises.

Model. – Three identical spherical colloidal microswimmers are labeled by $i = 1, 2, 3$, see fig. 1. Each carries a permanent magnetic dipole moment $\boldsymbol{m}_i$ of equal and constant magnitude m. The swimmers are linked by harmonic springs of spring constant k and finite equilibrium length $b > 0$. For simplicity, the springs are attached to the swimmer centers. In the equilibrium ground state, the colloidal molecule forms a linear straight object with the dipoles aligned along its axis. The Hamiltonian reads

$$\mathcal{H} = \frac{\mu_0 m^2}{4\pi} \sum_{\substack{i,j=1 \\ j<i}}^{3} \frac{\hat{\boldsymbol{m}}_i \cdot \hat{\boldsymbol{m}}_j - 3\left(\hat{\boldsymbol{m}}_i \cdot \hat{\boldsymbol{r}}_{ij}\right)\left(\hat{\boldsymbol{m}}_j \cdot \hat{\boldsymbol{r}}_{ij}\right)}{|\boldsymbol{r}_{ij}|^3} + \frac{k}{2} \sum_{i=1}^{2} \left(|\boldsymbol{r}_{i,i+1}| - b\right)^2 . \qquad (1)$$

Here, μ_0 denotes the vacuum permeability and $\hat{\boldsymbol{m}}_i = \boldsymbol{m}_i/m$. We refer to the swimmer positions as $\boldsymbol{R}_i = (x_i, y_i, z_i)$ in Cartesian coordinates. The distance vectors are given by $\boldsymbol{r}_{ij} = \boldsymbol{R}_j - \boldsymbol{R}_i$, and $\hat{\boldsymbol{r}}_{ij} = \boldsymbol{r}_{ij}/|\boldsymbol{r}_{ij}|$.

We consider low-Reynolds-number dynamics in an incompressible fluid. The swimmer bodies experience hydrodynamic couplings between each other. Their velocities $\boldsymbol{v}_i$ and angular velocities $\boldsymbol{\omega}_i$ result from all forces $\boldsymbol{F}_j = -\partial\mathcal{H}/\partial\boldsymbol{R}_j$ and torques $\boldsymbol{T}_j = -\hat{\boldsymbol{m}}_j \times (\partial\mathcal{H}/\partial\hat{\boldsymbol{m}}_j)$ on all swimmer bodies via the usual mobility matrices [39]:

$$\begin{pmatrix} \boldsymbol{v}_i \\ \boldsymbol{\omega}_i \end{pmatrix} = \sum_{j=1}^{3} \begin{pmatrix} \mu_{ij}^{tt} & \mu_{ij}^{tr} \\ \mu_{ij}^{rt} & \mu_{ij}^{rr} \end{pmatrix} \cdot \begin{pmatrix} \boldsymbol{F}_j \\ \boldsymbol{T}_j \end{pmatrix}. \qquad (2)$$

Up to second order in $1/|\boldsymbol{r}_{ij}|$, the mobility matrices read

$$\mu_{ij}^{tt} = \frac{1}{8\pi\eta|\boldsymbol{r}_{ij}|}\left(\mathsf{I} + \hat{\boldsymbol{r}}_{ij}\hat{\boldsymbol{r}}_{ij}\right) \quad \text{for } i \neq j, \quad \mu_{ii}^{tt} = \frac{\mathsf{I}}{6\pi\eta a}, \qquad (3)$$

$$\mu_{ij}^{tr} = \mu_{ij}^{rt} = \frac{1}{8\pi\eta}\frac{1}{|\boldsymbol{r}_{ij}|^2}\hat{\boldsymbol{r}}_{ij}\times \quad \text{for } i \neq j, \quad \mu_{ii}^{tr} = \mu_{ii}^{rt} = 0, \qquad (4)$$

$$\mu_{ij}^{rr} = 0 \quad \text{for } i \neq j, \quad \mu_{ii}^{rr} = \frac{\mathsf{I}}{8\pi\eta a^3}, \qquad (5)$$

where η is the viscosity of the surrounding fluid, a is the hydrodynamic radius of the swimmer bodies, I denotes the identity matrix, and $\hat{\boldsymbol{r}}_{ij}\hat{\boldsymbol{r}}_{ij}$ is a dyadic product. There is no summation over i and j in these expressions.

As noted above, each swimmer acts on the fluid via an active force dipole σ_i. We parameterize $\sigma_i = \sigma_0\left(\hat{\boldsymbol{m}}_i\hat{\boldsymbol{m}}_i - \mathsf{I}/3\right)$ [40], thus the forces point along and rotate together with $\pm\hat{\boldsymbol{m}}_i$. σ_0 sets the propulsion strength and the character of the propulsion mechanism. For $\sigma_0 < 0$ we use the term "puller" and for $\sigma_0 > 0$ the term "pusher". To achieve self-propulsion, the force dipoles σ_i are shifted out of the swimmer centers along $\hat{\boldsymbol{m}}_i$ by $\varepsilon > 0$ for pullers and $\varepsilon < 0$ for pushers, respectively, see fig. 1. In this way, isolated swimmers always propel into the direction $\hat{\boldsymbol{m}}_i$. As a result, to the above order, one obtains "active" contributions to the swimmer velocities [41,42]

$$\boldsymbol{v}_i^a = \sum_{j=1}^{3} \mu^{tt,a}(\boldsymbol{R}_i - \boldsymbol{R}_j - \varepsilon\hat{\boldsymbol{m}}_j) : \sigma_j, \qquad (6)$$

where $\mu^{tt,a}(\boldsymbol{r})$ is a third-rank tensor of the form

$$\mu^{tt,a}(\boldsymbol{r}) = \left(-\hat{\boldsymbol{r}}\mathsf{I} + 3\hat{\boldsymbol{r}}\hat{\boldsymbol{r}}\hat{\boldsymbol{r}}\right)/(8\pi\eta r^2). \qquad (7)$$

From now on, we measure all lengths in units of b, time t in units of $6\pi\eta a/k$, and energies in units of kb^2. Moreover, we introduce the dimensionless parameters $\tilde{a} = a/b$, $\tilde{\varepsilon} = \varepsilon/b$, $\tilde{\sigma} = 3\sigma_0\tilde{a}/2kb^2$, and $\tilde{m}^2 = m^2\mu_0/4\pi k b^5$. Altogether, since $\mathrm{d}\boldsymbol{R}_i/\mathrm{d}t = \boldsymbol{v}_i$ and $\mathrm{d}\hat{\boldsymbol{m}}_i/\mathrm{d}t = \boldsymbol{\omega}_i \times \hat{\boldsymbol{m}}_i$, we obtain the rescaled equations of motion

$$\frac{\mathrm{d}\boldsymbol{R}_i}{\mathrm{d}t} = -\frac{\partial\mathcal{H}}{\partial\boldsymbol{R}_i} - \frac{3\tilde{a}}{4}\sum_{\substack{j=1 \\ j\neq i}}^{3} \frac{1}{|\boldsymbol{r}_{ij}|}\left(\mathsf{I} + \hat{\boldsymbol{r}}_{ij}\hat{\boldsymbol{r}}_{ij}\right) \cdot \frac{\partial\mathcal{H}}{\partial\boldsymbol{R}_j} + \boldsymbol{v}_i^a - \frac{3\tilde{a}}{4}\sum_{\substack{j=1 \\ j\neq i}}^{3} \frac{\hat{\boldsymbol{r}}_{ij}}{|\boldsymbol{r}_{ij}|^2} \times \left(\hat{\boldsymbol{m}}_j \times \frac{\partial\mathcal{H}}{\partial\hat{\boldsymbol{m}}_j}\right) \qquad (8)$$

for the positions and

$$\frac{\mathrm{d}\hat{\boldsymbol{m}}_i}{\mathrm{d}t} = -\frac{3}{4\tilde{a}^2}\left(\hat{\boldsymbol{m}}_i \times \frac{\partial\mathcal{H}}{\partial\hat{\boldsymbol{m}}_i}\right) \times \hat{\boldsymbol{m}}_i - \frac{3\tilde{a}}{4}\sum_{j\neq i} \frac{1}{|\boldsymbol{r}_{ij}|^2}\left(\hat{\boldsymbol{r}}_{ij} \times \frac{\partial\mathcal{H}}{\partial\boldsymbol{R}_j}\right) \times \hat{\boldsymbol{m}}_i \qquad (9)$$

for the orientations.

At rest, *i.e.* for $\tilde{\sigma} = 0$, the molecule is straight and aligned due to the magnetic interactions, see fig. 2(a). When $\tilde{\sigma}$ is switched to nonzero values, the whole molecule starts to self-propel for $\tilde{\varepsilon} \neq 0$. Artificially, we can for any value of $\tilde{\sigma}$ delimit the molecule to the straight configuration by confining all swimmer positions and orientations to

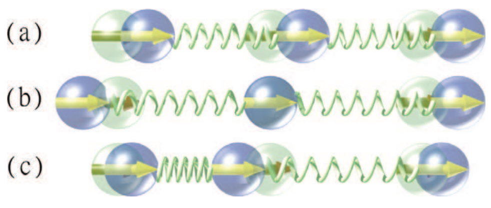

Fig. 2: (Color online) Sketch of the one-dimensional longitudinal deformation modes in the aligned straight configuration: (a) rigid translation, (b) extension or compression, (c) displacement of the center swimmer with respect to the outer ones. Lighter colors indicate the unperturbed state for reference.

a common axis, here the x-axis. The distances between the swimmers and the overall speed in the resulting steadily propelling straight state are calculated numerically, using a fourth-order Runge-Kutta scheme. We set the magnetic interactions $\tilde{m}$ small enough such that a magnetic collapse due to the attractive dipole interactions does not occur.

One isolated swimmer would propel with a speed $\tilde{\sigma}/\tilde{\varepsilon}^2$. Due to the hydrodynamic interactions, the collective speed of the overall straight molecule deviates from this value. Moreover, for pushers ($\tilde{\varepsilon} < 0$, $\tilde{\sigma} > 0$) the molecule elongates, while for pullers ($\tilde{\varepsilon} > 0$, $\tilde{\sigma} < 0$) it contracts when compared to the nonpropelling state. In both situations, due to the $\tilde{\varepsilon}$ shift, the distance between the front and center swimmers is larger than between the center and rear swimmers. For simplicity, we set $|\tilde{\varepsilon}| = \tilde{a}$ from now on.

Our scope is to determine the stability of the resulting steady straight configuration against small perturbations, as they may arise, *e.g.*, from imperfections in the system, thermal fluctuations, or perturbations from outside. We parameterize the swimmer positions as $\boldsymbol{R}_i(t) = (x_i(t) + \delta x_i(t), \delta y_i(t), \delta z_i(t))$ and the orientations of the magnetic moments as $\hat{\boldsymbol{m}}_i(t) = \big(1, \delta m_{i_y}(t), \delta m_{i_z}(t)\big)$ to linear order in the deviations $\delta x_i(t)$, $\delta y_i(t)$, $\delta z_i(t)$, $\delta m_{i_y}(t)$, and $\delta m_{i_z}(t)$ from the straight aligned configuration. Next, we linearize the system of eqs. (8) and (9) in these deviations. Summarizing all deviations ($i = 1, 2, 3$) in a 15-dimensional vector $\boldsymbol{\delta Q}(t)$, the resulting system of dynamic equations for the deviations has the form

$$\frac{\mathrm{d}\boldsymbol{\delta Q}(t)}{\mathrm{d}t} = \mathsf{M} \cdot \boldsymbol{\delta Q}(t). \tag{10}$$

The coefficient matrix M depends on $\tilde{\sigma}$ as it contains the swimmer separation distances in the unperturbed steady straight state. Using $\boldsymbol{\delta Q}(t) = \boldsymbol{\delta Q}_0 \exp(\lambda t)$, we obtain

$$\mathsf{M} \cdot \boldsymbol{\delta Q}_0(t) = \lambda\, \boldsymbol{\delta Q}_0(t). \tag{11}$$

Thus, the eigenvalues of M identify the relaxation rates of deviations from the straight configuration. The eigenvectors determine the possible corresponding deformational modes. Both were determined numerically [43].

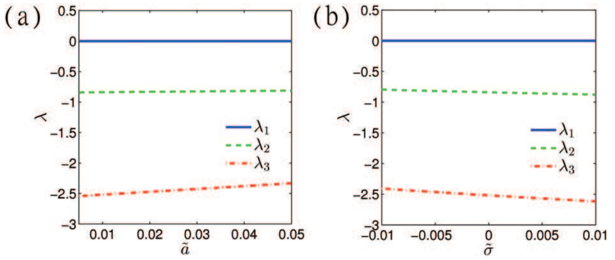

Fig. 3: (Color online) Influence of (a) swimmer size $\tilde{a}$ and (b) propulsion strength $\tilde{\sigma}$ on the relaxation of longitudinally perturbed aligned straight swimmer molecules. The rates λ_1, λ_2, λ_3 correspond to the modes depicted in fig. 2(a), (b), (c), respectively. Rigid translation is a zero mode, $\lambda_1 = 0$. Relaxation slows down with swimmer size $\tilde{a}$ and, for pullers, with propulsion strength $\tilde{\sigma} < 0$. It speeds up with $\tilde{\sigma} > 0$ for pushers. (Parameters: $\tilde{m}^2 = 0.005$, (a) $\tilde{\sigma} = 0$, (b) $\tilde{a} = 0.01$.)

Longitudinal perturbations. – First, we stick to the aligned straight configuration of the swimmer molecule and only consider longitudinal perturbations. That is, we set $\delta y_i, \delta z_i, \delta m_{i_y}, \delta m_{i_z} = 0$ and only allow deviations $\delta x_i(t)$ ($i = 1, 2, 3$). This offers a first insight into the role of the surrounding fluid and the active drive. The three resulting deformational modes (for not too high $|\tilde{\sigma}|$) qualitatively agree with those in the absence of self-propulsion and hydrodynamic interactions, see fig. 2. As expected, the translational mode (fig. 2(a)) represents a zero mode ($\lambda_1 = 0$), independently of the radius $\tilde{a}$ of the swimmer bodies and the propulsion strength $\tilde{\sigma}$, see fig. 3.

The relaxation of the two remaining modes, *i.e.* extension/compression of the whole swimmer molecule (fig. 2(b)) and displacements of the central swimmer with respect to the outer ones (fig. 2(c)), slows down with increasing swimmer size $\tilde{a}$. This is reflected by decreasing relaxation rates $|\lambda_2|$ and $|\lambda_3|$ in fig. 3(a). As a cause of this behavior, larger $\tilde{a}$ increase the friction with the surrounding fluid and enhance the hydrodynamic interaction between the swimmers. However, neighboring swimmers that tend to relax the deformation of their linking spring must move into opposite directions. Resulting fluid flows induced by one of the two swimmers oppose the motion of the other.

For increasing propulsion strength $|\tilde{\sigma}|$, the relaxation of perturbations speeds up for pushers ($\tilde{\sigma} > 0$) and slows down for pullers ($\tilde{\sigma} < 0$), see fig. 3(b). To understand this difference, we should recall eq. (7): the flow fields induced by the active force dipoles decay as r^{-2} with distance r. Thus, relaxations of compressed springs have more weight in determining the dependence on $\tilde{\sigma}$ than relaxations of extended springs. Naturally, the flow fields induced by pushers ($\tilde{\sigma} > 0$) support the separation process of two neighboring swimmers after they have come too close. This enhances the elongation of compressed linking springs. In contrast to that, the flow field induced by pullers ($\tilde{\sigma} < 0$) tends to drag the swimmers towards each other and thus hinders or slows down decompression of the springs.

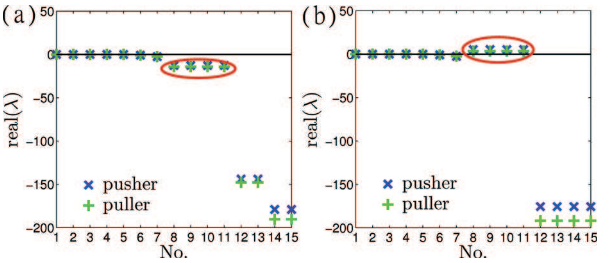

Fig. 4: (Color online) Real parts of the relaxation rates λ for (a) a stable case ($|\tilde{\sigma}| = 0.005$) and (b) an unstable situation ($|\tilde{\sigma}| = 0.01$). We first find five zero modes corresponding to rigid translations or rotations. The next two modes are identified as the one-dimensional longitudinal modes displayed in fig. 2(b), (c). Both, rotations and translations into the transverse directions, appear in the remaining eight modes. Out of these, the last four are dominated by rotational perturbations and relax much faster than the translational components in the intermediate modes. Those modes leading to destabilization at high $|\tilde{\sigma}|$ are marked by a loop. (Parameters: $\tilde{m}^2 = 0.005$, $\tilde{a} = 0.01$.)

Destabilization of the aligned straight state. – Finally, we analyze the stability of the straight configuration of the swimmer molecule against all possible perturbational degrees of freedom $\boldsymbol{\delta Q}$. This leads to 15 perturbational modes, resulting from the three spatial and two orientational degrees of freedom per swimmer. Typical relaxation spectra, *i.e.* the real parts of the relaxation rates λ, are shown in fig. 4. Naturally, five zero modes representing rigid translations and rotations emerge. Next, we find that longitudinal perturbations (see fig. 2(b), (c)) always decay. Apart from that, in the investigated regime, we observe the molecule to be stable against perturbations dominated by local rotations of the individual swimmers (the last four modes in fig. 4). Yet, with increasing propulsion strength $|\tilde{\sigma}|$, the molecule becomes linearly unstable against four intermediate perturbational modes, signaled by positive real parts of their eigenvalues λ. They are marked by the loop in fig. 4. Actually these modes form two pairs, resulting from the fact that there are two degenerate transverse directions.

For one of these two degenerate pairs, we plot the real parts of the eigenvalues λ as a function of the strength of self-propulsion $|\tilde{\sigma}|$ in fig. 5. At low propulsion strength $|\tilde{\sigma}|$, these λ are real and negative. Thus, small perturbations decay in a simple relaxation process. On the curves in fig. 5 this regime corresponds to the inner rounded parts. Interestingly, starting from the center of these curves, upon increase of $|\tilde{\sigma}|$, the straight configuration is first stabilized. The upper branch, corresponding to the less stable mode, drops towards lower $\lambda < 0$. At a certain $\tilde{\sigma}$, the two branches of $\lambda < 0$ meet. Beyond this point, the two relaxation rates form a complex conjugate pair. Then, the dynamic response of the swimmer molecule to the perturbations changes qualitatively. Perturbations now decay in an *oscillatory* way.

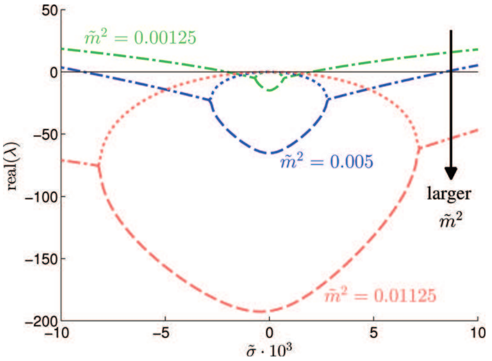

Fig. 5: (Color online) Real parts of the eigenvalues λ encircled in fig. 4, against which the straight aligned configuration first becomes unstable with increasing propulsion strength $|\tilde{\sigma}|$. Cases for different values of the magnetic interaction strength $\tilde{m}^2$ are depicted. Stronger magnetic interactions stabilize the straight state. Between the branching points, the relaxation rates λ are negative and real; beyond these points, they form a pair of complex conjugate eigenvalues. (Parameters: $\tilde{a} = 0.01$.)

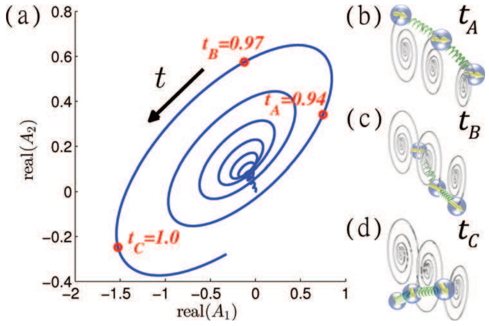

Fig. 6: (Color online) Oscillatory linear instability of a straight initial configuration, here for the case of pushers (qualitatively the same properties are observed for pullers). (a) Tracking the real parts of the amplitudes of the two degenerate unstable pairs of modes over time, real(A_1) and real(A_2), reveals the unstable oscillatory cycle that spirals outwards. (b)–(d) Illustration of the destabilized configurations at the times marked in (a). Spirals indicate the real-space trajectories of the individual microswimmers during destabilization in a comoving frame. For better visualization, rotations are enlarged by a relative factor of 4. (Parameters: $\tilde{m}^2 = 0.005$, $\tilde{a} = 0.01$, $\tilde{\sigma} = 0.01$.)

Further increasing $|\tilde{\sigma}|$ in fig. 5, the real parts of the eigenvalues λ become positive. Then, the straight aligned state is linearly unstable. The more the system is stabilized by magnetic interactions $\tilde{m}$, the later this happens. The instability is of an *oscillatory* type. Technically speaking, at the threshold of linear instability, the real parts of the pair of complex conjugate eigenvalues change sign, meeting the requirement for a *Hopf bifurcation* scenario [44].

Figure 6 illustrates the dynamics of the swimmer molecule during the oscillatory instability as predicted by the linear analysis. We numerically iterate the linearized dynamic equation (10) forward in time, starting from a weak perturbation of the straight initial state. At each

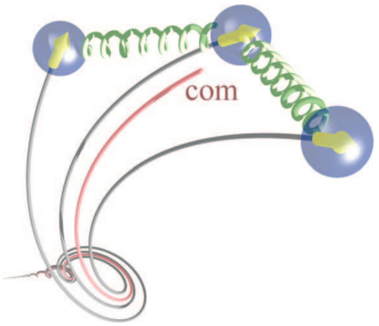

Fig. 7: (Color online) Example trajectory of the three-swimmer molecule in the linearly unstable regime after slight perturbation of the initially straight configuration. A corkscrew-like trajectory is observed for the individual swimmers and the center of mass (com). (Parameters: $\tilde{m}^2 = 0.005$, $\tilde{a} = 0.01$, $\tilde{\sigma} = 0.01$.)

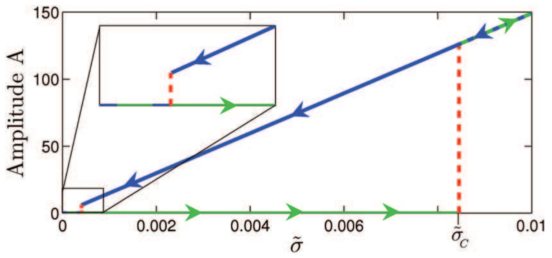

Fig. 8: (Color online) Hysteresis loop for the deviation from a straight configuration of the swimmer molecule, measured by the amplitude A (see text for the definition). The straight configuration becomes linearly unstable at $\tilde{\sigma} = \tilde{\sigma}_c$, where the amplitude jumps to finite values $A \neq 0$. Upon subsequent decrease of $\tilde{\sigma}$, the amplitude jumps back to $A = 0$ at $\tilde{\sigma} < \tilde{\sigma}_c$ as highlighted by the inset. (Parameters: $\tilde{m}^2 = 0.005$, $\tilde{a} = 0.01$.)

time step, we project the state of the whole molecule onto the unstable complex eigenmodes. This gives their amplitudes, which quantifies how these modes contribute to the present configuration. In the parametric plot of fig. 6(a), we track the configuration as a function of time: the abscissa and ordinate, respectively, indicate the real parts of the amplitudes of the two pairs of degenerate unstable eigenmodes. This plot demonstrates that i) the occupation of each of the two pairs of unstable eigenmodes, given by the abscissa and ordinate, respectively, oscillates over time; ii) the occupation oscillates between the two pairs of unstable eigenmodes, leading to the cycles; and iii) the system is unstable as the cycle spirals outwards. Figures 6(b)–(d) illustrate snapshots of the overall configuration during one cycle. The oscillatory cycle in fig. 6(a) shows up as spiral-like motions of the individual swimmers, although, in isolation, they perform straight rotation-free motions. An active torque is not explicitly imposed [45].

Strictly speaking, the linearized equation (10) can only predict the onset of the linear instability and describe the system behavior at low amplitudes just after destabilization. To further illustrate the motion beyond the instability, we numerically iterate the full nonlinear system of eqs. (8) and (9) forward in time. An example trajectory obtained in this way after slight perturbation of a straight initial configuration is depicted in fig. 7. There, the oscillatory instability is reflected in real space by a corkscrew-like trajectory of the whole swimmer molecule.

Finally, we wish to clarify the nature of the bifurcation. For this purpose, we numerically iterate eqs. (8) and (9) forward in time for varying propulsion strength $\tilde{\sigma}$. After each change in $\tilde{\sigma}$, we wait until a steady state is reached. The deviation from the straight configuration is quantified by an amplitude $A = [\sum_{i=1}^{3}(\Delta_{i,\parallel}^2 + \Delta_{i,\perp}^2)]^{1/2}$, where $\Delta_{i,\parallel}$ and $\Delta_{i,\perp}$ measure the longitudinal and transversal displacements of the swimmer bodies with respect to a steady straight configuration of the whole molecule. Increasing $\tilde{\sigma} \geq 0$ in fig. 8, we observe a jump to nonzero values of $A \neq 0$ at a value $\tilde{\sigma} = \tilde{\sigma}_c$ that agrees with the prediction of our linear stability analysis. Upon decreasing $\tilde{\sigma}$ again, the swimmer molecule returns to its straight configuration only at significantly lower values $\tilde{\sigma} < \tilde{\sigma}_c$. The system shows hysteretic behavior. Altogether, this signals a subcritical nature of the Hopf bifurcation.

Conclusions. – We have investigated the dynamic behavior of a linear magnetic microswimmer molecule. The colloidal molecule consists of three individual spherical self-propelled microswimmers, connected in a linear arrangement by elastic harmonic springs. These individual swimmers hydrodynamically interact with each other, with slight variations arising from pusher or puller propulsion mechanisms. Magnetic interactions support a straight configuration of the molecule. Yet, increasing the propulsion strength, the straight configuration is destabilized. As a central result, we find that the destabilization occurs in the form of an oscillatory instability, in accord with a subcritical Hopf bifurcation scenario. Hysteresis is observed as a function of the propulsion strength.

Our description can be extended in many ways, for instance by addressing more than three linked self-propelled particles [46] or different swimmer topologies, *e.g.* higher-dimensional objects [47] or ring-like structures [25,48]. Individual swimmers of varying sizes and propulsion strengths, direct correlations between swimmer rotations and their mutual distances [49], as well as the collective behavior of many interacting molecules may be analyzed. We further hope that our predictions will stimulate experimental investigations. Corresponding colloidal microswimmer molecules could, *e.g.*, be generated by linking magnetic self-propelled Janus particles [32] via DNA polymer chains [34]. The strength of self-propulsion can be tuned in light-controlled experiments [4]. Aspects of our results may further be important for the behavior of interacting magnetotactic bacteria [50,51]. More artificially, spring-like interactions between the constituents could be mimicked by caging them in comoving optical laser traps using feedback control loops [52].

* * *

The authors thank Giorgio Pessot for helpful discussions and the Deutsche Forschungsgemeinschaft for support through the SPP 1681.

REFERENCES

[1] Menzel A. M., *Phys. Rep.*, **554** (2015) 1.
[2] Elgeti J., Winkler R. G. and Gompper G., *Rep. Prog. Phys.*, **78** (2015) 056601.
[3] Jiang H.-R., Yoshinaga N. and Sano M., *Phys. Rev. Lett.*, **105** (2010) 268302.
[4] Buttinoni I., Volpe G., Kümmel F., Volpe G. and Bechinger C., *J. Phys.: Condens. Matter*, **24** (2012) 284129.
[5] Howse J. R., Jones R. A. L., Ryan A. J., Gough T., Vafabakhsh R. and Golestanian R., *Phys. Rev. Lett.*, **99** (2007) 048102.
[6] Theurkauff I., Cottin-Bizonne C., Palacci J., Ybert C. and Bocquet L., *Phys. Rev. Lett.*, **108** (2012) 268303.
[7] Berg H. C., *Nature*, **254** (1975) 389.
[8] Cates M. E., *Rep. Prog. Phys.*, **75** (2012) 042601.
[9] Romanczuk P., Bär M., Ebeling W., Lindner B. and Schimansky-Geier L., *Eur. Phys. J. ST*, **202** (2012) 1.
[10] Toner J. and Tu Y., *Phys. Rev. Lett.*, **75** (1995) 4326.
[11] Vicsek T., Czirók A., Ben-Jacob E., Cohen I. and Shochet O., *Phys. Rev. Lett.*, **75** (1995) 1226.
[12] Grégoire G. and Chaté H., *Phys. Rev. Lett.*, **92** (2004) 025702.
[13] Wensink H. H., Dunkel J., Heidenreich S., Drescher K., Goldstein R. E., Löwen H. and Yeomans J. M., *Proc. Natl. Acad. Sci. U.S.A.*, **109** (2012) 14308.
[14] Weber C. A., Hanke T., Deseigne J., Léonard S., Dauchot O., Frey E. and Chaté H., *Phys. Rev. Lett.*, **110** (2013) 208001.
[15] Menzel A. M. and Löwen H., *Phys. Rev. Lett.*, **110** (2013) 055702.
[16] Ferrante E., Turgut A. E., Dorigo M. and Huepe C., *New J. Phys.*, **15** (2013) 095011.
[17] Ferrante E., Turgut A. E., Dorigo M. and Huepe C., *Phys. Rev. Lett.*, **111** (2013) 268302.
[18] Menzel A. M., Ohta T. and Löwen H., *Phys. Rev. E*, **89** (2014) 022301.
[19] Manoharan V. N., Elsesser M. T. and Pine D. J., *Science*, **301** (2003) 483.
[20] van Blaaderen A., *Science*, **301** (2003) 470.
[21] Kraft D. J., Groenewold J. and Kegel W. K., *Soft Matter*, **5** (2009) 3823.
[22] Soto R. and Golestanian R., *Phys. Rev. Lett.*, **112** (2014) 068301.
[23] Soto R. and Golestanian R., *Phys. Rev. E*, **91** (2015) 052304.
[24] Liebchen B., Marenduzzo D., Pagonabarraga I. and Cates M. E., *Phys. Rev. Lett.*, **115** (2015) 258301.
[25] Kaiser A., Popowa K. and Löwen H., *Phys. Rev. E*, **92** (2015) 012301.
[26] Najafi A. and Golestanian R., *Phys. Rev. E*, **69** (2004) 062901.
[27] Golestanian R. and Ajdari A., *Phys. Rev. E*, **77** (2008) 036308.
[28] Günther S. and Kruse K., *EPL*, **84** (2008) 68002.
[29] Uchida N. and Golestanian R., *Phys. Rev. Lett.*, **106** (2011) 058104.
[30] Friedrich B. M. and Jülicher F., *Phys. Rev. Lett.*, **109** (2012) 138102.
[31] Bennett R. R. and Golestanian R., *New J. Phys.*, **15** (2013) 075028.
[32] Baraban L., Makarov D., Streubel R., Mönch I., Grimm D., Sanchez S. and Schmidt O. G., *ACS Nano*, **6** (2012) 3383.
[33] Tierno P., Güell O., Sagués F., Golestanian R. and Pagonabarraga I., *Phys. Rev. E*, **81** (2010) 011402.
[34] Dreyfus R., Baudry J., Roper M. L., Fermigier M., Stone H. A. and Bibette J., *Nature*, **437** (2005) 862.
[35] Ogrin F. Y., Petrov P. G. and Winlove C. P., *Phys. Rev. Lett.*, **100** (2008) 218102.
[36] Yeomans J. M., Pushkin D. O. and Shum H., *Eur. Phys. J. ST*, **223** (2014) 1771.
[37] Baskaran A. and Marchetti M. C., *Proc. Natl. Acad. Sci. U.S.A.*, **106** (2009) 15567.
[38] Menzel A. M., Saha A., Hoell C. and Löwen H., *J. Chem. Phys.*, **144** (2016) 024115.
[39] Reichert M. and Stark H., *Phys. Rev. E*, **69** (2004) 031407.
[40] Saintillan D., *Kinetic Models for Biologically Active Suspensions*, in *Natural Locomotion in Fluids and on Surfaces* (Springer, New York) 2012, pp. 53–71.
[41] Pozrikidis C., *Boundary Integral and Singularity Methods for Linearized Viscous Flow* (Cambridge University Press, Cambridge) 1992.
[42] Jayaraman G., Ramachandran S., Ghose S., Laskar A., Bhamla M. S., Kumar P. B. S. and Adhikari R., *Phys. Rev. Lett.*, **109** (2012) 158302.
[43] Eigen 3.2.4, `http://eigen.tuxfamily.org`.
[44] Cross M. C. and Hohenberg P. C., *Rev. Mod. Phys.*, **65** (1993) 851.
[45] Wada H. and Netz R. R., *EPL*, **75** (2006) 645.
[46] Kaiser A., Babel S., ten Hagen B., von Ferber C. and Löwen H., *J. Chem. Phys.*, **142** (2015) 124905.
[47] Küchler N., Löwen H. and Menzel A. M., *Phys. Rev. E*, **93** (2016) 022610.
[48] Messina R., Khalil L. A. and Stanković I., *Phys. Rev. E*, **89** (2014) 011202.
[49] Pessot G., Weeber R., Holm C., Löwen H. and Menzel A. M., *J. Phys.: Condens. Matter*, **27** (2015) 325105.
[50] Blakemore R., *Science*, **190** (1975) 377.
[51] Frankel R. B., Blakemore R. P. and Wolfe R. S., *Science*, **203** (1979) 1355.
[52] Kotar J., Leoni M., Bassetti B., Lagomarsino M. C. and Cicuta P., *Proc. Natl. Acad. Sci. U.S.A.*, **107** (2010) 7669.